van der Waals and retardation (Casimir) interactions of an electron or an atom with multilayered walls

Fei Zhou
245 Park Avenue, Room 2-429, Bear Stearns & Co. Inc., New York, New York 10167

Larry Spruch
Department of Physics, New York University, New York, New York 10003
(Received 26 September 1994)

We use the quantized surface mode technique to evaluate the interaction V of a "particle" (an electron or an atom) with two sets of plane parallel walls of arbitrary thicknesses and arbitrary permittivities; one set is on one side of the particle and the other set is on the other side. It is shown that a set of walls on either side of the particle can be treated as a single wall with an effective reflection coefficient $\mathcal{R}$, a function of the frequency and the angle of incidence of an incoming plane wave. The two sets of walls have thereby been effectively reduced to one wall on each side. Using a modified version of the standard image technique—the locations of the images are the usual ones, but the strengths are modified—one finds that the closed form for V can be reexpressed as a sum of interactions of the set of images on a given side with the wall on the other side. Taking various limits (thin walls, thick walls, metallic walls, dilute media) reproduces many known interactions and also provides a number of results not previously obtained. The latter results enable us to give quantitative estimates of the error incurred in approximating a wall of finite thickness by a wall of semi-infinite thickness or approximating a wall with large permittivity by a wall of infinite permittivity. In an attempt to make the paper user friendly, we provide a tabulation of many of the short-range (van der Waals–like) and long-range (retardation) interactions now known, with equation references.

PACS number(s): 31.30.Jv, 03.70.+k, 12.20.−m, 77.90.+k

I. INTRODUCTION

There have been many studies of the interactions of two plane semi-infinite parallel walls [1–3]. Our primary interest will be in the interaction with a wall or walls of an electron or a (polarizable) atom (or molecule), for separations ranging from a few Bohr radii to distances where retardation effects must be considered. One-wall cases include the interactions of an atom with an ideal wall [4], an atom and a semi-infinite dielectric wall [5] (obtained from the interaction of two semi-infinite dielectric walls by having one of the walls describable as a dilute gas of atoms), an electron with an ideal wall [6], and an electron with a semi-infinite dielectric wall [7] and with a semi-infinite dielectric permeable wall [8].

We will consider the interaction of an atom or an electron, placed between two walls, with the walls. The walls are separated by a distance l and have thicknesses d_1 and d_2 and (frequency-dependent) permittivities ϵ_1 and ϵ_2. The three regions separated by the two walls have permittivities ϵ_4, ϵ_3, and ϵ_5. (See Fig. 1. The odd labeling of the ϵ's is a consequence of an effort to use some of the same notation used in previous publications.) All permeabilities are taken to be unity. By appropriate choices of the various thicknesses and ϵ's of the five regions, we reproduce all of the results noted above and we also obtain some additional results. For example, for $d_2 = 0$ and $\epsilon_5 = \epsilon_3$, the two-wall system reduces to a one-wall system, while $d_1 = \infty$ gives a semi-infinite wall. We will examine various limits in detail. Of particular interest are conditions under which, to a given accuracy, a wall can be assumed to be infinitely thick, or a perfect conductor. The interaction when one or both of the walls have a permittivity close to unity often assumes a relatively simple form. Various results, including those of general types and those in certain limits, are summarized in the tables near the end of the paper. The results obtained can be most easily interpreted in terms of effective reflection coefficients [9]. This interpretation allows one to extend the results to an arbitrary number of layers of arbitrary thicknesses and permittivities. The multilayered results should be of interest for some systems in condensed matter physics and in biology.

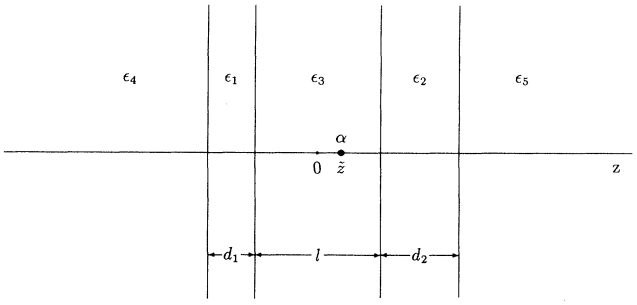

FIG. 1. The surfaces of the five media are parallel to the xy plane. The center plane of medium 3 is at $z = 0$. The system whose interaction is to be determined is characterized by its polarizability α and is positioned at $\tilde{z}$ in medium 3.

To lowest order, the approximation under consideration, the electron or the atom is affected by the field between the plates, but does not affect that field. The determination of the interaction is therefore reduced to the determination of that field. We choose to make that determination by using the very effective quantized surface mode technique [10]. (The quantized Fresnel mode technique [11], used in Refs. [7,8], is also a powerful technique, though the treatment of evanescent modes, modes propagating parallel to the surface of the walls and decaying exponentially in the outer regions, may require some further attention.)

It may be useful to collect at this point some comments on a few of the more frequently occurring symbols. Many will be defined more precisely below. Subscripts D, M, $\mathcal{D}$, at and el denote dielectric walls, metallic (ideal) walls, dilute walls, atoms, and electrons, respectively. The subscript α denotes a polarizable system, an atom or an electron, and V denotes an interaction. α in the text refers to the system, while α in an equation represents the frequency-dependent electric dipole polarizability of the system. Thus $V_{D_1\alpha D_2}$ is the interaction (over and above that of one set of walls with another set of walls) of system α, placed between two sets of walls, with the two sets. The symbols r, R, $\mathcal{R}$, $\mathcal{B}$, and β, with any subscripts or superscripts, are related to reflection coefficients. The superscript λ denotes a state of polarization of the electric field and the subscripts 1 through 5 often refer to a particular one of the five walls generally under consideration; l_1 and l_2, however, refer to the distances between α and walls 1 and 2. $\mathcal{A}_0$, for any symbol $\mathcal{A}$, denotes the value of $\mathcal{A}$ at zero frequency. ϵ is a permittivity and the superscripts vdW and ret on a potential V denote (short-range) van der Waals–like and (long-range) retarded interactions.

Throughout, we use the standard approximation of assuming that walls have perfectly well-defined plane surfaces. This approximation would not be adequate if the object with which it interacts—an electron, an atom, or a second wall—were within perhaps two or three Bohr radii, but we limit our considerations to rather larger separations. A nearby object does of course affect the internal structure of a wall. The adequacy of the model for the present level of experimental accuracy will be commented on very briefly at the end of Sec. IV.

II. QUANTIZED SURFACE MODES

The vacuum fluctuation fields can be determined for the system defined above. For our purposes we need consider only the zero-point energy associated with the surface modes, namely, those modes that are exponentially decaying in the outer regions, that is, for $z < -d_1 - l/2$ and $z > l/2 + d_2$. In general, the electric and the magnetic fields of the surface mode q can be written in the forms

$$\mathbf{E}_q = i\mathcal{N}e^{ik_x x + ik_y y}\left[a_q \mathbf{f}_q(z)e^{-i\omega t} - a_q^\dagger \mathbf{f}_q^*(z)e^{i\omega t}\right], \quad (2.1)$$

$$\mathbf{B}_q = \mathcal{N}e^{ik_x x + ik_y y}\left[a_q \mathbf{g}_q(z)e^{-i\omega t} + a_q^\dagger \mathbf{g}_q^*(z)e^{i\omega t}\right], \quad (2.2)$$

where $\mathcal{N} = (2\pi\hbar\omega/L^2)^{1/2}$ is the normalization factor, with L the length of the normalization box in the x and the y directions, and $\mathbf{k} = (k_x, k_y)$ is the propagation vector in the xy plane. [q denotes $\mathbf{k}$ *and* one of the two possible polarizations of the electromagnetic field. The fields are quantized and conform to the surface mode boundary conditions.] $a_q^\dagger$ and a_q are the usual creation and annihilation operators, respectively. The z-dependent functions satisfy the wave equations

$$\frac{d^2\mathbf{f}_{q,j}}{dz^2} - K_j^2 \mathbf{f}_{q,j} = \mathbf{0}, \quad (2.3)$$

$$\frac{d^2\mathbf{g}_{q,j}}{dz^2} - K_j^2 \mathbf{g}_{q,j} = \mathbf{0}, \quad (2.4)$$

where $j = 1, ..., 5$ denote one of the five regions and

$$K_j^2 = k^2 - \epsilon_j(\omega)\frac{\omega^2}{c^2}. \quad (2.5)$$

$\mathbf{f}_q$ and $\mathbf{g}_q$ are functions $\mathbf{k}$ and ω. We label the two independent states of the field by the superscript $\perp$ for the mode with the polarization of the electric field perpendicular to the plane formed by $\mathbf{k}$ and the z axis and by the superscript $\parallel$ for the mode with the polarization parallel to the plane formed by $\mathbf{k}$ and the z axis. For simplicity of the mode description, we choose the coordinates system in which $\mathbf{k}$ is parallel to the x axis. For the perpendicular mode, we then have

$$f_x^\perp = 0, \qquad f_{y,j}^\perp = A_j^\perp e^{K_j z} + B_j^\perp e^{-K_j z}, \qquad f_z^\perp = 0, \quad (2.6)$$

with $B_4 = A_5 = 0$ as required for the surface modes. Using $\boldsymbol{\nabla} \times \mathbf{E}_q = i(\omega/c)\mathbf{B}_q$, we find

$$g_x^\perp = i\frac{c}{\omega}\frac{df_y^\perp}{dz}, \qquad g_y^\perp = 0, \qquad g_z^\perp = \frac{c}{\omega}k f_y^\perp. \quad (2.7)$$

The boundary conditions associated with the mode $\perp$ are that $f_y^\perp$ and $df_y^\perp/dz$ are continuous. Applying these conditions to the solutions (2.3) at $z = -d_1 - l/2, -l/2, l/2$ and $l/2 + d_2$, we obtain, after some simple but lengthy algebra,

$$\left[1 - Q_1^\perp Q_2^\perp\right]_{\omega_N^\perp} = 0, \quad (2.8)$$

where

$$Q_1^\perp \equiv \frac{\rho_{13}^\perp - \rho_{14}^\perp e^{-2K_1 d_1}}{1 - \rho_{13}^\perp \rho_{14}^\perp e^{-2K_1 d_1}} e^{-K_3 l}, \quad (2.9)$$

$$Q_2^\perp \equiv \frac{\rho_{23}^\perp - \rho_{25}^\perp e^{-2K_2 d_2}}{1 - \rho_{23}^\perp \rho_{25}^\perp e^{-2K_2 d_2}} e^{-K_3 l}, \quad (2.10)$$

with

$$\rho_{mn}^\perp \equiv \frac{K_m - K_n}{K_m + K_n}. \quad (2.11)$$

The subscript $\omega_N^\perp$ in Eq. (2.8) denotes the allowed quantized frequencies of the perpendicular mode for fixed $\mathbf{k}$. Introducing

$$G^\perp \equiv G^\perp(\omega) \equiv 1 - Q_1^\perp Q_2^\perp, \tag{2.12}$$

we rewrite Eq. (2.8) as

$$G^\perp(\omega_N^\perp) = 0. \tag{2.13}$$

The electromagnetic energy associated with the mode $q = (\mathbf{k}, \omega_N^\perp)$ is the zero-point energy $\hbar\omega_N^\perp/2$, that is,

$$\left\langle 0 \left| \frac{1}{8\pi} \int d\mathbf{r} \left[\frac{d(\epsilon\omega)}{d\omega} |\mathbf{E}_q|^2 + |\mathbf{B}_q|^2 \right]_{\omega_N^\perp} \right| 0 \right\rangle = \frac{1}{2}\hbar\omega_N^\perp, \tag{2.14}$$

where $|0\rangle$ represents the vacuum photon state and the subscript $\omega_N^\perp$ indicates that the expression in square brackets is to be evaluated at one of the frequencies determined by Eq. (2.13). Notice the factor $d(\epsilon\omega)/d\omega$ rather than simply ϵ in the above expression; see Ref. [12] for an explanation. Direct evaluation of Eq. (2.14), with the aid of the boundary conditions, leads to

$$\sum_j \int_j dz \left[\left(\omega \frac{d\epsilon_j}{d\omega} + 2\epsilon_j \right) |f_{y,j}^\perp|^2 \right]_{\omega_N^\perp} = 2. \tag{2.15}$$

There is a term to term correspondence between the integral (2.15) and

$$\frac{dG^\perp}{d\omega} = \sum_j \frac{dK_j}{d\omega} \frac{dG^\perp}{dK_j} = \sum_j \frac{\omega}{c^2 K_j} \left(\frac{\omega}{2} \frac{d\epsilon_j}{d\omega} + \epsilon_j \right) \frac{dG^\perp}{dK_j}. \tag{2.16}$$

We can directly verify that

$$A_3^\perp B_3^\perp = - \left[\frac{\omega}{c^2 K_3 (dG^\perp/d\omega)} \right]_{\omega_N^\perp}. \tag{2.17}$$

In arriving at Eq. (2.17), we used the boundary conditions, expressed the coefficients $A_j^\perp$ and $B_j^\perp$ in terms of $A_3^\perp$ and $B_3^\perp$, and factored out $A_3^\perp B_3^\perp$ in evaluating Eq. (2.15). $A_3^\perp$ and $B_3^\perp$ are related through

$$\frac{A_3^\perp}{B_3^\perp} = -\frac{1}{(Q_1^\perp)_{\omega_N^\perp}} = -(Q_2^\perp)_{\omega_N^\perp}. \tag{2.18}$$

Analyses similar to those presented above can be applied to the parallel mode. For this mode, we have, for the electric fields, $f_y^\parallel = 0$,

$$f_{z,j}^\parallel = A_j^\parallel e^{K_j z} + B_j^\parallel e^{-K_j z}, \tag{2.19}$$

and

$$f_x^\parallel = -\frac{1}{ik} \frac{df_z^\parallel}{dz} \tag{2.20}$$

and, for the magnetic fields, $g_x^\parallel = g_z^\parallel = 0$ and

$$g_y^\parallel = \frac{\epsilon}{k} \frac{\omega^2}{c^2} f_z^\parallel. \tag{2.21}$$

The boundary conditions for the parallel mode are that $\epsilon f_z^\parallel$ and $df_z^\parallel/dz$ are continuous. Similar to Eq. (2.12), we have

$$G^\parallel \equiv G^\parallel(\omega) \equiv 1 - Q_1^\parallel Q_2^\parallel, \tag{2.22}$$

where $Q_1^\parallel$ and $Q_2^\parallel$ are defined in the same way as $Q_1^\perp$ and $Q_2^\perp$ in Eqs. (2.9) and (2.10), except for the $\rho_{mn}^\perp$ of Eq. (2.11) being replaced by

$$\rho_{mn}^\parallel = \frac{\epsilon_n K_m - \epsilon_m K_n}{\epsilon_n K_m + \epsilon_m K_n}. \tag{2.23}$$

Furthermore, in analogy to Eqs. (2.13), (2.17), and (2.18), we have

$$G^\parallel(\omega_N^\parallel) = 0, \tag{2.24}$$

$$A_3^\parallel B_3^\parallel = - \left[\frac{k^2 c^2}{\epsilon_3 \omega^2} \frac{\omega}{c^2 K_3 (dG^\parallel/d\omega)} \right]_{\omega_N^\parallel}, \tag{2.25}$$

and

$$\frac{A_3^\parallel}{B_3^\parallel} = -\frac{1}{(Q_1^\parallel)_{\omega_N^\parallel}} = -(Q_2^\parallel)_{\omega_N^\parallel}. \tag{2.26}$$

III. FORCE PER UNIT AREA BETWEEN TWO ARBITRARY SETS OF WALLS

We will first calculate the total zero-point energy per unit area V/L^2 associated with the quantized surface modes discussed in the preceding section and then evaluate the force per unit area F/L^2 between wall 1 and wall 2, using

$$\frac{F}{L^2} = -\frac{d}{dl} \left(\frac{V}{L^2} \right). \tag{3.1}$$

The total energy of the system is simply the sum of the zero-point energies of the surface modes,

$$V = \sum_{\mathbf{k},N} \frac{1}{2}\hbar\omega_N^\perp + \sum_{\mathbf{k},N} \frac{1}{2}\hbar\omega_N^\parallel. \tag{3.2}$$

Since the sum over $\mathbf{k}$ in the above expression is actually an integral, we make the replacement

$$\sum_{\mathbf{k}} \to \left(\frac{L}{2\pi} \right)^2 \int d\mathbf{k} = \left(\frac{L}{2\pi} \right)^2 \int_0^\infty 2\pi k dk \tag{3.3}$$

and rewrite Eq. (3.2) as

$$\frac{V}{L^2} = \frac{\hbar}{4\pi} \int_0^\infty dk k \left(\sum_N \omega_N^\perp + \sum_N \omega_N^\parallel \right). \tag{3.4}$$

To perform the sums over N, we consider the generalized argument theorem for a complex function $H(\omega)$ that is analytic on and inside a closed contour C

$$\frac{1}{2\pi i}\oint_C d\omega H(\omega)\frac{G'(\omega)}{G(\omega)} = \sum_N \mu_N H(\omega_N) - \sum_P \mu_P H(\omega_P), \tag{3.5}$$

where $G(\omega)$ is analytic and has no zeros on C and is analytic inside C except for poles. The prime on $G(\omega)$ represents the derivative with respect to the argument ω and the contour integral is counterclockwise. ω_N and ω_P denote the positions of zeros and poles, respectively, of the function $G(\omega)$ inside C. μ_N is the number of zeros at ω_N and μ_P is the number of poles at ω_P. In applying Eq. (3.5), we set $H(\omega)=\omega$, let $G(\omega)$ be the functions defined in Eqs. (2.12) and (2.22), and choose as the contour the full imaginary axis ($i\infty$ to $-i\infty$) plus the right semi-infinite circle. On noting that the contribution from the right semi-infinite circle vanishes and that $G^\perp$ and $G^\parallel$ do not have poles inside C, we can reexpress the energy per unit area in Eq. (3.4) as

$$\begin{aligned}\frac{V}{L^2} &= -\frac{\hbar}{8\pi^2 i}\int_0^\infty dkk\int_{-i\infty}^{i\infty} d\omega\omega\left(\frac{G^{\perp\prime}}{G^\perp}+\frac{G^{\parallel\prime}}{G^\parallel}\right) \\ &= \frac{\hbar}{4\pi^2}\int_0^\infty dkk\int_0^\infty d\xi\left[\ln G^\perp(i\xi)+\ln G^\parallel(i\xi)\right].\end{aligned} \tag{3.6}$$

In the last step we introduced the variable change $\omega = i\xi$, performed partial integrations, and used the fact that $G^\perp$ and $G^\parallel$ are even functions of ξ and vanish as $\xi\sim\infty$. Using

$$\frac{dG^\lambda}{dl} = 2K_3 Q_1^\lambda Q_2^\lambda, \tag{3.7}$$

with λ denoting $\perp$ or $\parallel$, we find the force per unit area given by Eq. (3.1) to be

$$\frac{F}{L^2} = -\frac{\hbar}{2\pi^2}\int_0^\infty dkk\int_0^\infty d\xi K_3 \times\left(\frac{Q_1^\perp Q_2^\perp}{1-Q_1^\perp Q_2^\perp}+\frac{Q_1^\parallel Q_2^\parallel}{1-Q_1^\parallel Q_2^\parallel}\right), \tag{3.8}$$

where the variable change $\omega = i\xi$, though implicit, is understood in the above expression.

The expression (3.8) may be rearranged in a form that, in certain limits, reduces to some known results. Following Lifshitz [5], we introduce a new variable p, defined by

$$k^2 = \epsilon_3\frac{\xi^2}{c^2}(p^2-1). \tag{3.9}$$

We have, accordingly,

$$K_j = \sqrt{\epsilon_3}s_j\frac{\xi}{c}, \tag{3.10}$$

where

$$s_j = \left(\frac{\epsilon_j}{\epsilon_3}-1+p^2\right)^{1/2}. \tag{3.11}$$

In particular, we have $s_3 = p$ and $K_3 = \sqrt{\epsilon_3}p\xi/c$. We rewrite Eq. (3.8) as

$$\frac{F}{L^2} = -\frac{\hbar}{2\pi^2 c^3}\int_0^\infty d\xi\xi^3\epsilon_3^{3/2}\int_1^\infty dpp^2 \times\left(\frac{R_1^\perp R_2^\perp}{1-R_1^\perp R_2^\perp}+\frac{R_1^\parallel R_2^\parallel}{1-R_1^\parallel R_2^\parallel}\right), \tag{3.12}$$

with

$$R_{1,2}^\lambda = \mathcal{R}_{1,2}^\lambda e^{-\sqrt{\epsilon_3}p\xi l/c}, \tag{3.13}$$

where $\mathcal{R}_{1,2}^\lambda$ are defined as

$$\mathcal{R}_1^\lambda \equiv \frac{r_{13}^\lambda - r_{14}^\lambda e^{-2\sqrt{\epsilon_3}s_1\xi d_1/c}}{1-r_{13}^\lambda r_{14}^\lambda e^{-2\sqrt{\epsilon_3}s_1\xi d_1/c}}, \tag{3.14}$$

$$\mathcal{R}_2^\lambda \equiv \frac{r_{23}^\lambda - r_{25}^\lambda e^{-2\sqrt{\epsilon_3}s_2\xi d_2/c}}{1-r_{23}^\lambda r_{25}^\lambda e^{-2\sqrt{\epsilon_3}s_2\xi d_2/c}}, \tag{3.15}$$

with

$$r_{mn}^\perp = \frac{s_m - s_n}{s_m + s_n}, \qquad r_{mn}^\parallel = \frac{\epsilon_n s_m - \epsilon_m s_n}{\epsilon_n s_m + \epsilon_m s_n}. \tag{3.16}$$

The above result is valid for two parallel walls with arbitrary thicknesses and permittivities. (The force between two dielectric slabs of finite thicknesses in a symmetric one-dimensional mode was evaluated previously [13].) In the limits $d_1, d_2 \to \infty$, R_1^λ and R_2^λ reduce to

$$\mathcal{R}_1^\lambda|_{d_1\to\infty} = r_{13}^\lambda, \tag{3.17}$$

$$\mathcal{R}_2^\lambda|_{d_2\to\infty} = r_{23}^\lambda. \tag{3.18}$$

The force per unit area given by Eq. (3.12) is then simplified and reads

$$\begin{aligned}\left.\frac{F}{L^2}\right|_{d_1,d_2\to\infty} &= -\frac{\hbar}{2\pi^2 c^3}\int_0^\infty d\xi\xi^3\epsilon_3^{3/2}\int_1^\infty dpp^2 \\ &\times\left\{\left[(r_{13}^\perp r_{23}^\perp)^{-1}e^{2\sqrt{\epsilon_3}p\xi l/c}-1\right]^{-1}\right. \\ &\left.+\left[(r_{13}^\parallel r_{23}^\parallel)^{-1}e^{2\sqrt{\epsilon_3}p\xi l/c}-1\right]^{-1}\right\},\end{aligned} \tag{3.19}$$

which is the force per unit area between two semi-infinite walls derived earlier [15]. For metallic walls, $r_{13}^\lambda r_{23}^\lambda = 1$ for $\lambda = \perp$ or $\parallel$, the integrals can then be done, and one arrives at

$$\frac{F}{A} = -\frac{\pi^2}{720}\frac{\hbar c}{l^4}, \tag{3.20}$$

the Casimir result. Correction associated with finite conductivity have been obtained [14].

The result (3.19) can also be rearranged in an equivalent form with a double variable contour integration [5]. This rearrangement is also applicable to the general expression (3.12). After doing so, we have

$$\frac{F}{L^2} = -\frac{\hbar}{2\pi^2 c^3}\mathrm{Re}\int_0^\infty d\omega\omega^3\epsilon_3^{3/2}\left(\int_1^0+\int_0^{i\infty}\right)dpp^2 \times\left(\frac{R_1^\perp R_2^\perp}{1-R_1^\perp R_2^\perp}+\frac{R_1^\parallel R_2^\parallel}{1-R_1^\parallel R_2^\parallel}\right)_{\xi=-i\omega}. \quad (3.21)$$

We note here that an approach based on the Fresnel mode description [7,11] would directly lead to the result (3.21), in which the integration of p over the range $(0,1)$ represents the contribution of the traveling Fresnel modes while the integration over the imaginary axis represents the contribution of the evanescent modes. Moreover, we note that $\mathcal{R}^\lambda_{1,2}|_{\xi=-i\omega}$ are the reflection coefficients of a plane wave incident at an angle $\theta=\cos^{-1}p$ from the medium 3 onto wall 1 (with wall 4 behind it) and wall 2 (with wall 5 behind it), respectively. This feature was recognized previously [9] in the case of interaction between two semi-infinite walls, where the relevant reflection coefficients are $r^\lambda_{1,2}$, and is to have been expected in the present context. We have performed the cumbersome algebra leading to the above equations not simply to confirm that expectation but also to obtain explicit expressions for $\mathcal{R}^\lambda_{1,2}$; those expressions are necessary if we are to be able to estimate the accuracy of an approximation in which a wall of finite thickness and/or large permittivity is taken to be semi-infinite and/or a perfect conductor. The analysis also makes it clear that, for the present purposes, the reflection coefficient is the only relevant property not just for two walls but for any number of walls. Assume, for example, that regions 2 and 5 are replaced by three regions, labeled 2, 5, and 7, with region 7 extending to infinity. Region 2 would then be treated as was done above, while regions 5 and 7 would be treated as regions 2 and 5 were treated above, that is, by replacing them by a single region with the appropriate effective reflection coefficient; the analysis of the three-region problem would thereby be reduced to the analysis of a two-region problem.

As another limiting case we assume that the two walls are very thin and are immersed in a common medium ($\epsilon_3=\epsilon_4=\epsilon_5$); R_1^λ and R_2^λ defined in Eqs. (3.14) and (3.15) can then be approximated by

$$\mathcal{R}^\lambda_1|_{d_1\sim 0}\sim(2\sqrt{\epsilon_3}s_1\xi d_1/c)\frac{r^\lambda_{13}}{1-r^{\lambda\,2}_{13}}, \quad (3.22)$$

$$\mathcal{R}^\lambda_2|_{d_2\sim 0}\sim(2\sqrt{\epsilon_3}s_2\xi d_2/c)\frac{r^\lambda_{23}}{1-r^{\lambda\,2}_{23}} \quad (3.23)$$

and Eq. (3.12) simplifies to

$$\left.\frac{F}{L^2}\right|_{d_{1,2}\sim 0} \quad (3.24)$$

$$\sim -\frac{2\hbar d_1 d_2}{\pi^2 c^5}\int_0^\infty d\xi\xi^5\epsilon_3^{5/2}\int_1^\infty dpp^2 s_1 s_2 e^{-2\sqrt{\epsilon_3}p\xi l/c} \times\left[\frac{r^\perp_{13}r^\perp_{23}}{(1-r^{\perp\,2}_{13})(1-r^{\perp\,2}_{23})}+\frac{r^\parallel_{13}r^\parallel_{23}}{(1-r^{\parallel\,2}_{13})(1-r^{\parallel\,2}_{23})}\right].$$

If one wall is thin ($d_1\sim 0$) and the other is thick ($d_2\sim\infty$) and the former is surrounded by the same medium ($\epsilon_3=\epsilon_4$), the force per unit area becomes

$$\left.\frac{F}{L^2}\right|_{d_1\sim 0,d_2\sim\infty} \sim -\frac{\hbar d_1}{\pi^2 c^4}\int_0^\infty d\xi\xi^4\epsilon_3^2\int_1^\infty dp \times p^2 s_1 e^{-2\sqrt{\epsilon_3}p\xi l/c}\left(\frac{r^\perp_{13}r^\perp_{23}}{1-r^{\perp\,2}_{13}}+\frac{r^\parallel_{13}r^\parallel_{23}}{1-r^{\parallel\,2}_{13}}\right). \quad (3.25)$$

In the above discussion, "thin" and "thick" are relative to other parameters in the problem. The separation of the walls l serves as the primary criterion, though other parameters, such as ϵ_j, also play a role. Some analysis in this regard will be offered in the following section.

IV. INTERACTION BETWEEN TWO SETS OF WALLS WITH A POLARIZABLE SYSTEM IN BETWEEN

A. General result

A spherically symmetric, polarizable system with polarizability $\alpha(\omega)$ is placed at the position $\tilde{z}$ between wall 1 and wall 2, that is, in region 3. The simplest situation is that for which $\epsilon_3=1$, in which case $\alpha(\omega)$ is the polarizability of the system in isolation. Formally, the analysis does not change form if $\epsilon_3\neq 1$, though one must now know $\alpha(\omega)$ for the system embedded in the dielectric; at least for ϵ_3-1 small, one would often be able to make a reasonable estimate of the correction to the value of $\alpha(\omega)$ in isolation. We will therefore proceed with ϵ_3 arbitrary. Furthermore, we will allow system α to be an atom or an electron, since the analysis is initially of the same form for either case. Before obtaining the final results, however, we must sharply distinguish between the two cases. Thus, for example, for α far from either wall, its interaction is dominated by contributions from very low frequencies and the polarizability $\alpha(\omega)$ of an atom can be approximated by $\alpha(0)\equiv\alpha_0$. This approximation cannot be made for an electron, however, for which α_0 is infinite. Furthermore, the center of an atom is fixed, while the location of an electron whose interaction is being determined is not. For the above reasons, in the study of electron interactions we will always ultimately set $\epsilon_3=1$. Other than for ideal walls, we will further restrict our attention, in studies of an electron, to long-range interactions.

In the dipole approximation—in which the size of the system is neglected—the interaction between the particle and the walls can be expressed as

$$V_{D_1\alpha D_2}=\sum_q\langle 0|-\tfrac{1}{2}\alpha(\omega)\mathbf{E}_q^2|0\rangle. \quad (4.1)$$

The wall-wall interaction is unaffected by the introduction of the polarizable system, which is affected by, but does not affect, the field between the walls. $\mathbf{E}_q$ in Eq.

(4.1) represents the quantized electric field given in Eq. (2.1). The mode analyses in Sec. II enable us to replace the sum of modes in Eq. (4.1) by

$$\sum_q \to \left(\frac{L}{2\pi}\right)^2 \int_0^\infty dk 2\pi k \left(\sum_{\omega_N^\perp} + \sum_{\omega_N^\parallel}\right). \tag{4.2}$$

Straightforward evaluation of Eq. (4.1) yields

$$V_{D_1\alpha D_2} = -\frac{\hbar}{2}\int_0^\infty dkk \left(\sum_N \omega_N^\perp \alpha(\omega_N^\perp)|\mathbf{f}_3^\perp|^2 + \sum_N \omega_N^\parallel \alpha(\omega_N^\parallel)|\mathbf{f}_3^\parallel|^2\right), \tag{4.3}$$

where $\mathbf{f}_3^\perp$ and $\mathbf{f}_3^\parallel$ are defined and discussed in Sec. II. From Eqs. (2.6), (2.17), and (2.18), we find

$$|\mathbf{f}_3^\perp|^2 = |f_{y,3}^\perp|^2 = -\left[\frac{\omega I^\perp}{c^2 K_3 (dG^\perp/d\omega)}\right]_{\omega_N^\perp}, \tag{4.4}$$

with

$$I^\perp = 2Q_1^\perp Q_2^\perp - (Q_1^\perp e^{-2K_3\tilde{z}} + Q_2^\perp e^{2K_3\tilde{z}}), \tag{4.5}$$

and, from Eqs. (2.19), (2.20), (2.25), and (2.26), we find

$$|\mathbf{f}_3^\parallel|^2 = |f_{x,3}^\parallel|^2 + |f_{z,3}^\parallel|^2 = -\left[\frac{\omega I^\parallel}{c^2 K_3 (dG^\parallel/d\omega)}\right]_{\omega_N^\parallel}, \tag{4.6}$$

with

$$I^\parallel = 2Q_1^\parallel Q_2^\parallel - \left(1 + \frac{2K_3^2 c^2}{\epsilon_3 \omega^2}\right)(Q_1^\parallel e^{-2K_3\tilde{z}} + Q_2^\parallel e^{2K_3\tilde{z}}). \tag{4.7}$$

Substituting Eqs. (4.4) and (4.6) into Eq. (4.3), we obtain

$$V_{D_1\alpha D_2} = \frac{\hbar}{2c^2}\int_0^\infty dkk \left\{\sum_N \left[\alpha(\omega)\frac{\omega^2 I^\perp}{K_3 G^{\perp\prime}}\right]_{\omega_N^\perp} + \sum_N \left[\alpha(\omega)\frac{\omega^2 I^\parallel}{K_3 G^{\parallel\prime}}\right]_{\omega_N^\parallel}\right\}. \tag{4.8}$$

As we did for Eq. (3.4) in Sec. III, we perform the sum over N by using the generalized argument theorem (3.5). Using the same contour C as defined earlier, we obtain

$$V_{D_1\alpha D_2} = \frac{\hbar}{2\pi c^2}\int_0^\infty dkk \int_0^\infty d\xi \alpha(i\xi)\frac{\xi^2}{K_3} \times \left(\frac{I^\perp}{1 - Q_1^\perp Q_2^\perp} + \frac{I^\parallel}{1 - Q_1^\parallel Q_2^\parallel}\right). \tag{4.9}$$

(We point out here that the straightforward use of the argument theorem in the derivation of $V_{D_1\alpha D_2}$, as well as its use in the derivation of F/L^2 in Sec. III, is not mathematically rigorous. We will not concern ourselves with the related technical details involved. For an explanation of this inadequacy and the way to avoid it, see Ref. [2] and the references therein.) With the variable change introduced in Eq. (3.9), we reexpress Eq. (4.9) as

$$V_{D_1\alpha D_2} = \frac{\hbar}{2\pi c^3}\int_0^\infty d\xi \xi^3 \epsilon_3^{1/2}\alpha \int_1^\infty dp \times \left(\frac{J^\perp}{1 - R_1^\perp R_2^\perp} + \frac{J^\parallel}{1 - R_1^\parallel R_2^\parallel}\right), \tag{4.10}$$

where

$$J^\perp = 2R_1^\perp R_2^\perp - (R_1^\perp e^{-b} + R_2^\perp e^{b}), \tag{4.11}$$

$$J^\parallel = 2R_1^\parallel R_2^\parallel - (1 - 2p^2)(R_1^\parallel e^{-b} + R_2^\parallel e^{b}), \tag{4.12}$$

with

$$b = 2\sqrt{\epsilon_3} p\xi\tilde{z}/c. \tag{4.13}$$

Although the two sets of walls we considered in the above derivation consist of two layers of media each, the generality of the result (4.10) can be extended to multilayer walls. It was pointed out in Sec. III that $\mathcal{R}_{1,2}^\lambda$ represent overall reflection coefficients of the two-layer walls. For multilayer walls, we may simply replace the two-layer $\mathcal{R}_{1,2}^\lambda$ in Eq. (4.10) by the corresponding multilayer $\mathcal{R}_{1,2}^\lambda$. Note that the $\mathcal{R}_{1,2}^\lambda$ defined in Eqs. (3.14) and (3.15) are expressed iteratively; the $\mathcal{R}_{1,2}^\lambda$ of an $(n+1)$-layer wall could be expressed in terms of the $\mathcal{R}_{1,2}^\lambda$ of an n-layer wall and the $\mathcal{R}_{1,2}^\lambda$ of a semi-infinite one-layer wall.

The general expression (4.10) encompasses some well-known results and some not previously obtained. Various limits of the general results obtained above will be elaborated upon in the following.

To obtain the interaction with only one set of walls, we let $d_2 = 0$ and $\epsilon_3 = \epsilon_5$; we then have $\mathcal{R}_2^\lambda = 0$ and Eq. (4.10) reduces to

$$V_{D_1\alpha} = -\frac{\hbar}{2\pi c^3}\int_0^\infty d\xi \xi^3 \epsilon_3^{1/2}\alpha \int_1^\infty dp \times \left[\mathcal{R}_1^\perp + (1 - 2p^2)\mathcal{R}_1^\parallel\right] e^{-2\sqrt{\epsilon_3} p\xi l_1/c}, \tag{4.14}$$

where $\mathcal{R}_1^\lambda$ is defined in Eq. (3.14) and

$$l_1 = \frac{l}{2} + \tilde{z} \tag{4.15}$$

is the distance between the system α and the nearest of the single set of walls. The general result (4.10) for two walls can be reexpressed in a form with a sum of terms almost identical to the result (4.14) for one wall interactions. Using the fact that

$$\frac{1}{1 - R_1^\lambda R_2^\lambda} = \sum_{n=0}^\infty (R_1^\lambda R_2^\lambda)^n, \tag{4.16}$$

we rewrite Eq. (4.10) as

$$V_{D_1\alpha D_2} = \frac{\hbar}{2\pi c^3}\int_0^\infty d\xi\xi^3\epsilon_3^{1/2}\alpha\int_1^\infty dp\left\{\left(\frac{2R_1^\perp R_2^\perp}{1-R_1^\perp R_2^\perp}+\frac{2R_1^\parallel R_2^\parallel}{1-R_1^\parallel R_2^\parallel}\right)\right. \tag{4.17}$$
$$-\sum_{n=0}^\infty\left[\mathcal{R}_1^\perp(\mathcal{R}_1^\perp\mathcal{R}_2^\perp)^n+(1-2p^2)\mathcal{R}_1^\parallel(\mathcal{R}_1^\parallel\mathcal{R}_2^\parallel)^n\right]e^{-2\sqrt{\epsilon_3}p\xi l_n^+/c}$$
$$\left.-\sum_{n=0}^\infty\left[\mathcal{R}_2^\perp(\mathcal{R}_1^\perp\mathcal{R}_2^\perp)^n+(1-2p^2)\mathcal{R}_2^\parallel(\mathcal{R}_1^\parallel\mathcal{R}_2^\parallel)^n\right]e^{-2\sqrt{\epsilon_3}p\xi l_n^-/c}\right\},$$

where

$$l_n^\pm=\left(n+\frac{1}{2}\right)l\pm\tilde{z} \tag{4.18}$$

are the positions of the multiple images of the system α formed by the two surfaces at $\pm l/2$. [Note from Eq. (4.15) that $l_1 = l_0^+$.] The first term of Eq. (4.17) is independent of the position $\tilde{z}$. The second and third terms are in the same form as that of one-wall interaction (4.14), with l_1 replaced by $l_n^\pm$ and α by the corresponding $\alpha(\mathcal{R}_1^\lambda\mathcal{R}_2^\lambda)^n$. Therefore, we may view the interaction between α and two sets of walls as a sum of interactions between $\alpha(\mathcal{R}_1^\lambda\mathcal{R}_2^\lambda)^n$ at corresponding image positions and one set of walls. (See Fig. 2.) We will examine this relation in certain limits, where the expression (4.17) can be simplified. Consider a special case in which the left wall, denoted by the subscript $\mathcal{D}$, is semi-infinite and consists of a dilute medium ($d_1=\infty, \epsilon_1-1\equiv\delta_1\ll 1$), the right wall is metallic ($\epsilon_2=\infty$), and the system α resides in a vacuum ($\epsilon_3=1$). We then have

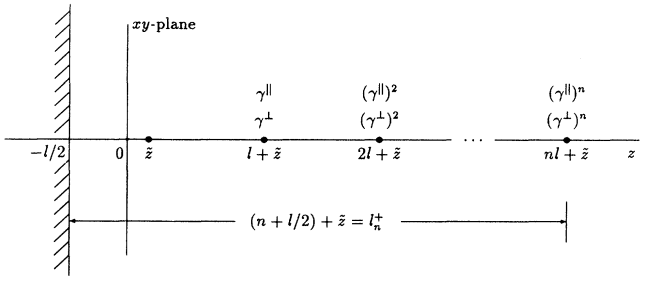

FIG. 2. By a comparison with Eq. (4.14), each term in the first infinite sum in Eq. (4.17) can be interpreted as the interaction of a system identical to the true polarizable system with a wall. As seen by the nth system, the fields, with polarization vectors characterized by $\perp$ and $\parallel$, are reduced (by virtue of multiple reflections) relative to the $n=0$ system by factors $(\gamma^\perp)^n$ and $(\gamma^\parallel)^n$, respectively, where $\gamma^\lambda=\mathcal{R}_1^\lambda\mathcal{R}_2^\lambda\exp(-2\epsilon_3^{1/2}p\xi l/c)$. The nth system is located at $nl+\tilde{z}$ and the surface of the semiinfinite wall with which it interacts is at $z=l/2$; the separation between the nth system and the wall is therefore $(nl+\tilde{z})+l/2$, or l_n^+. We indicate the locations of the systems and of the surface of the wall and the reduction factors for the fields. A similar interpretation applies to the second infinite sum in Eq. (4.17).

$$\mathcal{R}_1^\perp|_{d_1\to\infty,\epsilon_1\sim1,\epsilon_3=1}\sim\frac{\delta_1}{4p^2},$$
$$\mathcal{R}_1^\parallel|_{d_1\to\infty,\epsilon_1\sim1,\epsilon_3=1}\sim\frac{(1-2p^2)\delta_1}{4p^2},$$
$$\mathcal{R}_2^\perp|_{\epsilon_2=\infty,\epsilon_3=1}=1,\qquad\mathcal{R}_2^\parallel|_{\epsilon_2=\infty,\epsilon_3=1}=-1. \tag{4.19}$$

Through order δ_1, the sum in Eq. (4.17) reduces to a sum of finite terms

$$V_{\mathcal{D}\alpha M}=\frac{\hbar}{2\pi c^3}\int_0^\infty d\xi\xi^3\alpha\int_1^\infty dp$$
$$\times\left[\delta_1 e^{-2p\xi l/c}-2p^2e^{-2p\xi l_0^-/c}\right. \tag{4.20}$$
$$\left.-\delta_1\frac{1-2p^2+2p^4}{2p^2}(e^{-2p\xi l_0^+/c}+e^{-2p\xi l_1^-/c})\right].$$

The first term is $\tilde{z}$ independent. The second term represents the interaction between α and the metallic wall. [See Eq. (4.44) below.] The last term can be interpreted as the interactions of the dilute medium with α (l_0^+ is the distance between α and the surface of that wall) and with the image of α in the metallic wall (l_1^- is the distance between the image and that surface).

If the walls closest to α are both metallic, that is, if $\epsilon_1=\epsilon_2=\infty$, $\alpha(\mathcal{R}_1^\lambda\mathcal{R}_2^\lambda)^n$ reduces to just α. Then the sums in Eq. (4.17) bear a direct resemblance to the standard image interpretation. We will further discuss this in connection with the evaluation of V_{MatM} later in the section. The form given in Eq. (4.17) provides a simple picture of the origin of $V_{D_1\alpha D_2}$, but for computational purposes one would normally use Eq. (4.10).

If walls 1 and 2 are identical ($d_1=d_2\equiv d$ and $\epsilon_1=\epsilon_2\equiv\epsilon$) and the regions 3, 4, and 5 are filled with the same medium ($\epsilon_3=\epsilon_4=\epsilon_5$), the general form (4.10) reduces to

$$V_{D\alpha D}=\frac{\hbar}{\pi c^3}\int_0^\infty d\xi\xi^3\epsilon_3^{1/2}\alpha\int_1^\infty dp \tag{4.21}$$
$$\times\left[\frac{R^{\perp 2}-R^\perp\cosh(2\nu z/l)}{1-R^{\perp 2}}\right.$$
$$\left.+\frac{R^{\parallel 2}-(1-2p^2)R^\parallel\cosh(2\nu z/l)}{1-R^{\parallel 2}}\right],$$

where

$$R^\lambda = \mathcal{R}^\lambda e^{-\nu} \equiv \frac{r^\lambda(1-e^{-2\nu sd/pl})}{1-r^{\lambda 2}e^{-2\nu sd/pl}}e^{-\nu}, \tag{4.22}$$

with

$$\nu = \sqrt{\epsilon_3}p\xi l/c, \tag{4.23}$$

$$r^\perp = \frac{s-p}{s+p}, \qquad r^\parallel = \frac{\epsilon_3 s-\epsilon p}{\epsilon_3 s+\epsilon p}, \tag{4.24}$$

and

$$s = \left(\frac{\epsilon}{\epsilon_3}-1+p^2\right)^{1/2}. \tag{4.25}$$

Equations (4.22)–(4.24) are just simplified versions of Eqs. (3.13)–(3.16).

For a polarizable system interacting with only one wall, the general expression (4.10) can be greatly simplified. (The extension to one set of walls is straightforward.) We may either set $d_2 = 0$ and $\epsilon_3 = \epsilon_5$ or let $l = \infty$, and we also have $\epsilon_3 = \epsilon_4 \equiv \epsilon$. Either approach gives

$$V_{D\alpha} = -\frac{\hbar}{2\pi c^3}\int_0^\infty d\xi\xi^3\epsilon_3^{1/2}\alpha\int_1^\infty dp \times\left[\mathcal{R}^\perp+(1-2p^2)\mathcal{R}^\parallel\right]e^{-2\sqrt{\epsilon_3}p\xi l_1/c}, \tag{4.26}$$

where $\mathcal{R}^\perp$ and $\mathcal{R}^\parallel$ are defined in Eq. (4.22) and l is defined in Eq. (4.15).

In the following subsections, we will apply $V_{D\alpha D}$ of Eq. (4.21) and $V_{\alpha D}$ of Eq. (4.26) to an atom and then to an electron. Various limiting results, some known and many not previously obtained, will be discussed.

B. Wall-atom-wall interaction

V_{DatD} from Eq. (4.21) is valid for arbitrary l and $\tilde{z}$ (for $|\tilde{z}| \le l/2$). [We assume that $d_1 = d_2 \equiv d$, $\epsilon_1 = \epsilon_2 \equiv \epsilon$, and $\epsilon_3 = \epsilon_4 = \epsilon_5$, necessary conditions for the validity of Eq. (4.21).] As noted earlier, we will allow the medium in which the atom resides to have a permittivity ϵ_3 other than unity. For the atom, whose center is fixed, the result would seem to be formally correct if one uses for $\alpha(\omega)$ the polarizability in the presence of the dielectric. The retention of ϵ_3, for $\epsilon_3 \neq 1$, would presumably be an improvement for $\epsilon_3 \approx 1$.

There are two limits of particular interest, the first when $l/2 \pm \tilde{z}$—the distances of the atom from the walls—are both large and the second when l is small. V_{DatD}, under the former condition, gives the long-range retardation interaction, while under the latter condition it gives the short-range interaction of the van der Waals type.

For the long-range case, the contribution from frequencies near zero dominates. Thus the permittivities of the walls and the polarizability of the atom can be approximated by their static values

$$\epsilon \approx \epsilon(0) \equiv \epsilon_0, \quad \epsilon_3 \approx \epsilon_3(0) \equiv \epsilon_{30}, \quad \alpha \approx \alpha(0) \equiv \alpha_0. \tag{4.27}$$

Correspondingly, we approximate any quantity depending on ϵ and ϵ_3 by its static value

$$\mathcal{A}(\epsilon,\epsilon_3) \approx \mathcal{A}_0 = \mathcal{A}(\epsilon_0,\epsilon_{30}). \tag{4.28}$$

$\mathcal{A}$ in our analysis may represent s, $\mathcal{R}^\lambda$ and r^λ and later $\mathcal{B}$ and β. Making the above approximations in Eq. (4.21) and changing the variable from ξ to ν [see Eq. (4.23)], we obtain the retarded interaction for a wall-atom-wall system

$$V_{DatD}^{\rm ret} = \frac{\hbar c\alpha_0}{\pi l^4\epsilon_{30}^{3/2}}\int_0^\infty d\nu\nu^3\int_1^\infty\frac{dp}{p^4}\Psi(\mathcal{R}_0^\perp,\mathcal{R}_0^\parallel), \tag{4.29}$$

with

$$\Psi(\mathcal{R}_0^\perp,\mathcal{R}_0^\parallel) = \frac{\mathcal{R}_0^{\perp 2}e^{-2\nu}-\mathcal{R}_0^\perp e^{-\nu}\cosh(2\nu\tilde{z}/l)}{1-\mathcal{R}_0^{\perp 2}e^{-2\nu}} + \frac{\mathcal{R}_0^{\parallel 2}e^{-2\nu}-(1-2p^2)\mathcal{R}_0^\parallel e^{-\nu}\cosh(2\nu\tilde{z}/l)}{1-\mathcal{R}_0^{\parallel 2}e^{-2\nu}}. \tag{4.30}$$

There are two limits of special interest. For thick walls ($d \to \infty$), $\mathcal{R}^\lambda$ defined in Eq. (4.22) approaches r^λ and, accordingly, $\mathcal{R}_0^\lambda$ in Eq. (4.29) can be replaced by r_0^λ, that is,

$$V_{DatD}^{\rm ret}|_{d\to\infty} = \frac{\hbar c\alpha_0}{\pi l^4\epsilon_{30}^{3/2}}\int_0^\infty d\nu\nu^3\int_1^\infty\frac{dp}{p^4}\Psi(r_0^\perp,r_0^\parallel). \tag{4.31}$$

For thin walls ($d \sim 0$), $\mathcal{R}^\lambda$ can be approximated by

$$\mathcal{R}^\lambda \approx \frac{2s\nu d}{pl}\frac{r^\lambda}{1-r^{\lambda 2}}. \tag{4.32}$$

Since $\mathcal{R}_0^\lambda$ is a small quantity, we can simplify the interaction (4.29) to

$$V_{DatD}^{\rm ret}|_{d\sim 0} = -\frac{2\hbar c\alpha_0 d}{\pi l^5\epsilon_{30}^{3/2}}\psi\int_0^\infty d\nu\nu^4 e^{-\nu}\cosh(2\nu\tilde{z}/l), \tag{4.33}$$

where ψ, which depends only on ϵ_0/ϵ_{30}, is given by

$$\psi = \int_0^\infty dp\frac{s_0}{p^5}\left[\frac{r_0^\perp}{1-r_0^{\perp 2}}+(1-2p^2)\frac{r_0^\parallel}{1-r_0^{\parallel 2}}\right]. \tag{4.34}$$

Carrying out the integration over ν we obtain

$$V_{DatD}^{\rm ret}|_{d\sim 0} = -\frac{3\hbar c\alpha_0 d}{4\pi\epsilon_{30}^{3/2}}\left(\frac{1}{l_1^5}+\frac{1}{l_2^5}\right)\psi, \tag{4.35}$$

where $l_1 = l_0^+$ and $l_2 = l_0^-$ [defined in Eq. (4.18)] are the distances of the atom from the left wall and from the right wall, respectively. Since the interaction of an atom with a thin wall is weak, it is hardly surprising that the interaction of an atom with two thin walls is the sum of independent atom-wall interactions.

Note though that the individual terms in Eq. (4.35) fall off as $1/l_1^5$ and $1/l_2^5$, while for metallic walls or thick

dielectric walls a retarded wall-atom interaction falls off as the fourth power of the separation [4,15]. Corrections of order d/l_1 and d/l_2, which account for the different dependence on the separation, are to be expected from consideration of the effective thickness of the wall, the thickness which contains the atoms whose (long-range) contributions to the retarded interactions dominate. The effective thickness for a thin dielectric wall is the actual thickness d, but is proportional to l (with a coefficient small compared to unity) for a thick dielectric wall. A more formal analysis of the correction associated with a wall of finite thickness will be presented in Sec. IV F.

In contrast, for the short-range case (l small) significant contributions come from the region $\nu \sim 1$ in Eq. (4.21). [Consider Eq. (4.22) for R^λ. The $\exp(-\nu)$ factor is very small for $\nu \gg 1$, while the $1-\exp(2\sqrt{\epsilon_3}s\xi d/c)$ or $1-\exp(2\nu sd/pl)$ factor vanishes as $\nu \sim 0$.] $\nu \sim 1$ corresponds to $p \sim c/(\sqrt{\epsilon_3}\xi l) \gg 1$. Then, for ϵ/ϵ_3 of order unity, we can use the approximation $s \approx p$, which leads to

$$\mathcal{R}^\perp \approx 0, \qquad \mathcal{R}^\parallel \approx \mathcal{B} \equiv \beta \frac{1-e^{-2\nu d/l}}{1-\beta^2 e^{-2\nu d/l}}, \tag{4.36}$$

with

$$\beta \equiv \frac{\epsilon_3 - \epsilon}{\epsilon_3 + \epsilon}. \tag{4.37}$$

β is simply the reflection coefficient for a plane electromagnetic wave traveling in a region with permittivity ϵ incident normally on a semi-infinite medium with permittivity ϵ_3. A similar interpretation can be given to $\mathcal{B}$ for a medium of thickness d. Making the above approximations, changing the variable from p to ν in Eq. (4.21) and keeping only the leading l^{-3} term (which is the term associated with the factor $-2p^2$), we obtain the short-range van der Waals interaction for the wall-atom-wall system

$$V_{DatD}^{vdW} = \frac{2\hbar}{\pi l^3}\int_0^\infty d\nu \nu^2 \int_0^\infty d\xi \frac{\alpha}{\epsilon_3}\frac{\mathcal{B}e^{-\nu}\cosh(2\nu\tilde{z}/l)}{1-\mathcal{B}^2 e^{-2\nu}}. \tag{4.38}$$

Furthermore, for thick walls ($d \to \infty$), $\mathcal{B}$ in Eq. (4.38) can be approximated by β according to Eq. (4.36). Therefore, we have

$$V_{DatD}^{vdW}|_{d\to\infty} = \frac{2\hbar}{\pi l^3}\int_0^\infty d\nu \nu^2 \int_0^\infty d\xi \times \frac{\alpha}{\epsilon_3}\frac{\beta e^{-\nu}\cosh(2\nu\tilde{z}/l)}{1-\beta^2 e^{-2\nu}}. \tag{4.39}$$

On the other hand, if the walls are thin ($d \sim 0$), $\mathcal{B}$ can be approximated by

$$\mathcal{B}|_{d\sim 0} \approx \frac{2\nu d}{l}\frac{\beta}{1-\beta^2} = \frac{\nu d}{2l}\frac{(\epsilon_3{}^2-\epsilon^2)}{\epsilon_3\epsilon}. \tag{4.40}$$

The integral over ν can then be performed and the interaction (4.38) reduces to

$$V_{DatD}^{vdW}|_{d\sim 0} \sim \frac{3\hbar d}{16\pi}\left(\frac{1}{l_1^4}+\frac{1}{l_2^4}\right)\int_0^\infty d\xi \frac{\alpha}{\epsilon_3}\frac{(\epsilon_3{}^2-\epsilon^2)}{\epsilon_3\epsilon}. \tag{4.41}$$

[Just as for the long-range retarded interaction for thin walls, given in Eq. (4.35), the short-range result for thin walls is the sum of independent atom-wall interactions and the interactions differ from those for thick dielectrics (or metals) by corrections proportional to d_1/l and d_2/l.]

In the case of *ideal* walls we have the limiting values

$$\epsilon \to \infty, \qquad \mathcal{R}^\perp \to 1, \qquad \mathcal{R}^\parallel \to -1. \tag{4.42}$$

The interaction (4.21) then reduces to

$$V_{M\alpha M} = \frac{2\hbar}{\pi c^3}\int_0^\infty d\xi \xi^3 \epsilon_3^{1/2}\alpha \int_1^\infty dp \times \left[\frac{e^{-2\nu}-p^2 e^{-\nu}\cosh(2\nu\tilde{z}/l)}{1-e^{-2\nu}}\right]; \tag{4.43}$$

recall that the subscript M denotes a metallic wall. Correspondingly, the one-wall interaction Eq. (4.14) reduces to

$$V_{M\alpha} = -\frac{\hbar}{\pi c^3}\int_0^\infty d\xi \xi^3 \epsilon_3^{1/2}\alpha \int_1^\infty dp p^2 e^{-2\sqrt{\epsilon_3}p\xi l_1/c}. \tag{4.44}$$

The two-wall interaction (4.43) can be reexpressed in a form similar to (but simpler than) Eq. (4.17) by expanding $[1-\exp(-2\nu)]^{-1}$ in the $p^2\exp(-\nu)\cosh(2\nu\tilde{z}/l)$ term. One obtains

$$V_{M\alpha M} = \frac{2\hbar}{\pi c^3}\int_0^\infty d\xi \xi^3 \epsilon_3^{1/2}\alpha \int_1^\infty dp \left[\frac{e^{-2\nu}}{1-e^{-2\nu}} - \frac{p^2}{2}\sum_{n=0}^\infty (e^{-2\sqrt{\epsilon_3}p\xi l_n^+/c}+e^{-2\sqrt{\epsilon_3}p\xi l_n^-/c})\right], \tag{4.45}$$

where the $l_n^\pm$ are defined in Eq. (4.18). Apart from the z-independent term, that containing ν, $V_{M\alpha M}$ is just a sum of interactions between α at its multiple image positions and a single wall [compare with $V_{M\alpha}$ in Eq. (4.44)].

For the long-range interaction, we use the approximations (4.28) in (4.43) and change variables from ξ to ν. The integral over p can then be easily performed. For the resulting ν integral, we use

$$\int_0^\infty \frac{d\nu\nu^3}{e^{2\nu}-1} = \frac{\pi^4}{240}, \tag{4.46}$$

$$\int_0^\infty d\nu\nu^3 \frac{\cosh(2\nu\tilde{z}/l)}{\sinh(\nu)} = \pi^4 \frac{3-2\cos^2(\pi\tilde{z}/l)}{8\cos^4(\pi\tilde{z}/l)} \tag{4.47}$$

and find

$$V_{MatM}^{ret} = \frac{\pi^3\hbar c\alpha_0}{l^4\epsilon_{30}^{3/2}}\left[\frac{1}{360}-\frac{3-2\cos^2(\pi\tilde{z}/l)}{8\cos^4(\pi\tilde{z}/l)}\right] \tag{4.48}$$

or, equivalently,

$$V_{MatM}^{\rm ret} = \frac{3\hbar c\alpha_0}{8\pi\epsilon_{30}^{3/2}}\left[\frac{\pi^4}{135l^4} - \sum_{n=0}^{\infty}\left(\frac{1}{l_n^{+4}} + \frac{1}{l_n^{-4}}\right)\right]. \quad (4.49)$$

The second version is most easily derived from Eq. (4.45), once again using (4.28) and changing variables from ξ to ν [see Eq. (4.23)]; it is interpreted as a sum of image interactions. Apart from the trivial (formal) generalization from $\epsilon_3 = 1$ to ϵ_3 arbitrary and a reinterpretation of α_0 as the zero-frequency polarizability of the atom when within the medium, Eq. (4.48) is a result previously derived [16].

For the short-range interaction, we change variables from p to ν in Eq. (4.43). The approximations allowed under the assumption that l is arbitrarily small are much more readily understood by a physical argument than by a mathematical analysis. Thus, for $l \sim 0$, the time of flight cannot be relevant and we can let $c \to \infty$. The z-independent first term in the square bracket in Eq. (4.43) vanishes as $c \to \infty$ and in the second term the integration limits on ν, $\sqrt{\epsilon_3}\xi l/c$ to ∞, can be replaced by 0 to ∞, the difference vanishing as $c \to \infty$. We thereby obtain the nonrelativistic van der Waals–like result, with the characteristic l^{-3} behavior,

$$V_{MatM}^{\rm vdW} = -\frac{\hbar}{\pi l^3}T(\tilde{z}/l)\int_0^{\infty} d\xi \frac{\alpha}{\epsilon_3}, \quad (4.50)$$

with

$$T(\tilde{z}/l) = \int_0^{\infty} d\nu\nu^2 \frac{\cosh(2\nu\tilde{z}/l)}{\sinh(\nu)}. \quad (4.51)$$

As for the retarded interaction, the short-range interaction of Eq. (4.50) is a trivial formal generalization (from $\epsilon_3 = 1$ to ϵ_3 arbitrary, but with the reinterpretation of the polarizability not simply at zero frequency but at all frequencies, for the atom within the medium) of a previously derived result [16]. Corresponding to Eq. (4.48) in the long-range case, $V_{MatM}^{\rm vdW}$ can be reexpressed, on evaluating $T(\tilde{z}/l)$ by writing $1/(2\sinh\nu)$ as $\exp(-\nu) + \exp(-3\nu) + \cdots$, as

$$V_{MatM}^{\rm vdW} = -\frac{\hbar}{4\pi}\sum_{n=0}^{\infty}\left(\frac{1}{l_n^{+3}} + \frac{1}{l_n^{-3}}\right)\int_0^{\infty} d\xi\frac{\alpha}{\epsilon_3}, \quad (4.52)$$

which is a sum of wall-image interactions.

C. Wall-atom interaction

Analyses parallel to those leading to the results for the wall-atom-wall system can be applied to the much simpler expression (4.26) for the atom-wall system and the results are simpler as well. Here we record the corresponding long-range and short-range results

$$V_{Dat}^{\rm ret} = -\frac{\hbar c\alpha_0}{2\pi l_1^4\epsilon_{30}^{3/2}}\int_0^{\infty} d\nu\nu^3 e^{-2\nu}\int_1^{\infty}\frac{dp}{p^4} \times\left[\mathcal{R}_0^{\perp *} + (1-2p^2)\mathcal{R}_0^{\parallel *}\right], \quad (4.53)$$

$$V_{Dat}^{\rm vdW} = \frac{\hbar}{\pi l_1^3}\int_0^{\infty} d\nu\nu^2 e^{-2\nu}\int_0^{\infty} d\xi\frac{\alpha}{\epsilon_3}\mathcal{B}^*, \quad (4.54)$$

where $\mathcal{R}_0^{\lambda *}$ and $\mathcal{B}^*$ are defined in the same way as $\mathcal{R}_0^{\lambda}$ of Eq. (4.22) and $\mathcal{B}$ of Eq. (4.36), respectively, except that l in Eqs. (4.22) and (4.36) is replaced by l_1, the distance between the atom and the wall defined in Eq. (4.15). For a thick wall ($d \to \infty$), Eqs. (4.53) and (4.54) become

$$V_{Dat}^{\rm ret}|_{d\to\infty} = -\frac{3\hbar c\alpha_0}{16\pi l_1^4\epsilon_{30}^{3/2}}\int_1^{\infty}\frac{dp}{p^4}\left[r_0^{\perp} + (1-2p^2)r_0^{\parallel}\right], \quad (4.55)$$

$$V_{Dat}^{\rm vdW}|_{d\to\infty} = \frac{\hbar}{4\pi l_1^3}\int_0^{\infty} d\xi\frac{\alpha}{\epsilon_3}\frac{\epsilon_3-\epsilon}{\epsilon_3+\epsilon}, \quad (4.56)$$

while for a thin wall ($d \sim 0$), they become

$$V_{Dat}^{\rm ret}|_{d\sim 0} = -\frac{3\hbar c\alpha_0 d}{4\pi l_1^5\epsilon_{30}^{3/2}}\psi, \quad (4.57)$$

$$V_{Dat}^{\rm vdW}|_{d\sim 0} = \frac{3\hbar d}{16\pi l_1^4}\int_0^{\infty} d\xi\frac{\alpha}{\epsilon_3}\frac{\epsilon_3^2-\epsilon^2}{4\epsilon_3\epsilon}, \quad (4.58)$$

where ψ is given in Eq. (4.34). While the interactions (4.55) and (4.56) for a semi-infinite wall have been studied [15], the results (4.53) and (4.54) for the finite wall [including the results (4.57) and (4.58) in the thin wall limits] have not been available previously. Equations (4.53) and (4.54) can be used to deduce the Casimir and van der Waals interactions between two atoms; following Lifshitz [5], one simply takes the wall to be a dilute gas of atoms.

For an ideal wall, a direct reduction of Eq. (4.26) using the limiting values (4.42) gives

$$V_{M\alpha} = -\frac{\hbar}{\pi c^3}\int_0^{\infty} d\xi\xi^3\epsilon_3^{1/2}\alpha\int_1^{\infty} dpp^2 e^{-2\sqrt{\epsilon_3}p\xi l_1/c}. \quad (4.59)$$

Replacing $\epsilon_3^{1/2}$ and α by their zero-frequency values and integrating over ξ and then over p we obtain

$$V_{Mat}^{\rm ret} = -\frac{3\hbar c\alpha_0}{8\pi l_1^4\epsilon_{30}^{3/2}}. \quad (4.60)$$

Integrating over p and letting $c \to \infty$ gives

$$V_{Mat}^{\rm vdW} = -\frac{\hbar}{4\pi l_1^3}\int_0^{\infty} d\xi\frac{\alpha}{\epsilon_3}. \quad (4.61)$$

The result (4.60) is well known [4] and the result (4.61) for $\epsilon_3 = 1$ has also been studied [6].

D. Wall-electron-wall interaction

We now consider an electron between two identical walls; in line with an earlier discussion we set $\epsilon_3 = 1$. Substituting polarizability of a free electron, associated with its time-dependent displacement generated by an

electric field of frequency ω [with ω in $\alpha(\omega) = -e^2/m_e\omega^2$ replaced by $i\xi$]

$$\alpha(i\xi) = \frac{e^2}{m_e\xi^2} \tag{4.62}$$

into the general expression (4.21), we obtain

$$V_{DelD} = \frac{\hbar e^2}{\pi m_e c^3}\int_0^\infty d\xi\xi\int_1^\infty dp\Theta, \tag{4.63}$$

where

$$\Theta = \sum_{\lambda=\perp,\parallel}\frac{R^{\lambda 2} - R^\lambda\cosh(2\nu\tilde{z}/l)}{1-R^{\lambda 2}} + 2p^2\frac{R^\parallel\cosh(2\nu\tilde{z}/l)}{1-R^{\parallel 2}}. \tag{4.64}$$

The last term in Θ needs special attention, for it could seem to cause the p integrals to diverge if analyses parallel to those used for the wall-atom-wall interactions were used. To bypass this difficulty, we follow a procedure used previously for a similar situation [7] and introduce

$$\bar{\Theta} \equiv \Theta - 2p^2\frac{\mathcal{B}e^{-\nu}\cosh(2\nu\tilde{z}/l)}{1-\mathcal{B}^2e^{-2\nu}}, \tag{4.65}$$

where $\mathcal{B}$ is defined in Eq. (4.36). As will be seen below, the decomposition given in Eq. (4.65) avoids the divergence mentioned above; adding and subtracting the term involving $\mathcal{B}$, the contributions from $\bar{\Theta}$ and from the $\mathcal{B}$ terms separately converge. Accordingly, we may rewrite the wall-electron-wall interaction (4.63) as

$$V_{DelD} = V_{DelD,I} + V_{DelD,II}, \tag{4.66}$$

with

$$V_{DelD,I} = \frac{\hbar e^2}{\pi m_e c^3}\int_0^\infty d\xi\xi\int_1^\infty dp\bar{\Theta}, \tag{4.67}$$

$$V_{DelD,II} = \frac{2\hbar e^2}{\pi m_e c^3}\int_0^\infty d\xi\xi\int_1^\infty dpp^2\frac{\mathcal{B}e^{-\nu}\cosh(2\nu\tilde{z}/l)}{1-\mathcal{B}^2e^{-2\nu}}. \tag{4.68}$$

$V_{DelD,I}$ given by Eq. (4.67) can then be treated in the same manner as that used for V_{DatD} in Sec. VI B. In the long-range case, we use the approximations (4.28) and obtain

$$V^{\rm ret}_{DelD,I} = \frac{\hbar e^2}{\pi m_e cl^2}\int_0^\infty d\nu\nu\int_1^\infty\frac{dp}{p^2}\bar{\Theta}_0, \tag{4.69}$$

where

$$\bar{\Theta}_0 = \sum_{\lambda=\perp,\parallel}\frac{\mathcal{R}_0^{\lambda 2}e^{-2\nu} - \mathcal{R}_0^\lambda e^{-\nu}\cosh(2\nu\tilde{z}/l)}{1-\mathcal{R}_0^{\lambda 2}e^{-2\nu}} + 2p^2\left(\frac{\mathcal{R}_0^\parallel e^{-\nu}}{1-\mathcal{R}_0^{\parallel 2}e^{-2\nu}} - \frac{\mathcal{B}_0e^{-\nu}}{1-\mathcal{B}_0^2e^{-2\nu}}\right)\cosh(2\nu\tilde{z}/l). \tag{4.70}$$

[See Eq. (4.28) for the meaning of subscript zero.] We note from Eq. (4.36) that for $p \sim \infty$

$$\mathcal{R}^\parallel \approx \mathcal{B} - \frac{\mathcal{B}}{2p^2}, \tag{4.71}$$

which ensures the convergence of the p integral of the second term in Eq. (4.70). This is achieved at the expense of having to evaluate an additional contribution $V_{DelD,II}$ given in Eq. (4.68). To analyze $V_{DelD,II}$ we first follow the procedure of double contour integration mentioned in Sec. II and rewrite Eq. (4.68), valid for the short- and the long-range cases, as

$$V_{DelD,II} = \frac{2\hbar e^2}{\pi m_e c^3}\mathrm{Re}\int_0^{i\infty} d\xi\xi\left(\int_1^0 + \int_0^{i\infty}\right)dpp^2 \times\frac{\mathcal{B}e^{-\nu}\cosh(2\nu\tilde{z}/l)}{1-\mathcal{B}^2e^{-2\nu}}. \tag{4.72}$$

In the long-range case, we use the approximation (4.28). Since $\mathcal{B}_0$ is real, we can neglect the contribution from the p integration along the imaginary axis. After changing the variables from ξ to ν [see Eq. (4.23)] and performing the integration along the path 1 to 0, we obtain

$$V^{\rm ret}_{DelD,II} = -\frac{2\hbar e^2}{\pi m_e cl^2}\int_0^\infty d\nu\nu\frac{\mathcal{B}_0e^{-\nu}\cosh(2\nu\tilde{z}/l)}{1-\mathcal{B}_0^2e^{-2\nu}}. \tag{4.73}$$

[In obtaining Eq. (4.73), we have also performed a contour integration down along the positive imaginary ν axis ($i\infty$ to 0), then along the positive real axis (0 to ∞), and then along the upper-right one-quarter infinite circle (∞ to $i\infty$).] Combining the results (4.69) and (4.73), we obtain the total long-range wall-electron-wall interaction

$$V^{\rm ret}_{DelD} = \frac{\hbar e^2}{\pi m_e cl^2}\int_0^\infty d\nu\nu\int_1^\infty\frac{dp}{p^2}\Phi(\mathcal{R}_0^\perp,\mathcal{R}_0^\parallel,\mathcal{B}_0), \tag{4.74}$$

with

$$\Phi(\mathcal{R}_0^\perp,\mathcal{R}_0^\parallel,\mathcal{B}_0) = \bar{\Theta}_0 - \frac{2\mathcal{B}_0e^{-\nu}\cosh(2\nu\tilde{z}/l)}{1-\mathcal{B}_0^2e^{-2\nu}}. \tag{4.75}$$

For thick walls, $V^{\rm ret}_{DelD}$ can be simplified for one can replace $\mathcal{R}_0^\lambda$ and $\mathcal{B}_0$ in Eq. (4.75) by r_0^λ and β_0, respectively. [See Eqs. (4.24) and (4.37) for the definitions of r^λ and β.] As a result, we have

$$V^{\rm ret}_{DelD}|_{d\to\infty} = \frac{\hbar e^2}{\pi m_e cl^2}\int_0^\infty d\nu\nu\int_1^\infty\frac{dp}{p^2}\Phi(r_0^\perp,r_0^\parallel,\beta_0). \tag{4.76}$$

For thin walls, we can use the approximations (4.32) and (4.40). Then, following a procedure similar to that leading to Eq. (4.35), we obtain

$$V^{\rm ret}_{DelD}|_{d\sim 0} = \frac{\hbar e^2 d}{4\pi m_e c}\left(\frac{1}{l_1^3}+\frac{1}{l_2^3}\right)\phi, \tag{4.77}$$

with

$$\phi = -\frac{2\beta_0}{1-\beta_0^2} + \int_1^\infty dp \left[-\frac{s_0}{p^3}\left(\frac{r_0^\perp}{1-{r_0^\perp}^2} + \frac{r_0^\parallel}{1-{r_0^\parallel}^2}\right) + \frac{2s_0 r_0^\parallel/p}{1-{r_0^\parallel}^2} - \frac{2\beta_0}{1-\beta_0^2}\right]. \quad (4.78)$$

For ideal walls, we use the limiting values (4.42) and rewrite the interaction (4.63) as

$$V_{MelM} = \frac{2\hbar e^2}{\pi m_e c^3}\left[\int_0^\infty d\xi\xi \int_1^\infty dp \frac{e^{-2\nu}}{1-e^{-2\nu}} + \mathrm{Re}\int_0^{i\infty} d\xi\xi \int_0^1 dp p^2 \frac{e^{-\nu}\cosh(2\nu\tilde{z}/l)}{1-e^{-2\nu}}\right]. \quad (4.79)$$

The second term in the above expression is associated with the second term in Eq. (4.64) with a double contour integration applied [5]. This term can now be treated in the same manner as that used in arriving at (4.72). After doing so, we reduce Eq. (4.79) to

$$V_{MelM} = \frac{2\hbar e^2}{\pi m_e c l^2}\int_0^\infty d\nu\nu\left[\frac{1}{e^{2\nu}-1} + \frac{\cosh(2\nu\tilde{z}/l)}{2\sinh(\nu)}\right]. \quad (4.80)$$

Using

$$\int_0^\infty \frac{d\nu\nu}{e^{2\nu}-1} = \frac{\pi^2}{24}, \quad (4.81)$$

$$\int_0^\infty d\nu\nu \frac{\cosh(2\nu\tilde{z}/l)}{\sinh(\nu)} = \frac{\pi^2}{4\cos^2(\pi\tilde{z}/l)}, \quad (4.82)$$

we recover the known result [6]

$$V_{MelM} = \frac{\hbar e^2}{\pi m_e c l^2}\left[\frac{1}{12} + \frac{1}{4\cos^2(\pi\tilde{z}/l)}\right]. \quad (4.83)$$

E. Wall-electron interaction

Substituting Eq. (4.62) into Eq. (4.26), we have the interaction between an electron and a wall

$$V_{Del} = -\frac{\hbar e^2}{2\pi m_e c^3}\int_0^\infty d\xi\xi \int_1^\infty dp \times \left[\mathcal{R}^{\perp *} + (1-2p^2)\mathcal{R}^{\parallel *}\right] e^{-2p\xi l_1/c}. \quad (4.84)$$

Similar but simpler analyses than those used above for the wall-electron-wall system can be applied to the wall-electron interaction (4.84) for various limiting results, which can also be deduced from the corresponding wall-electron-wall results by taking the limit $l \to \infty$. Without further discussion, we record the long-range interaction

$$V_{Del}^{ret} = -\frac{\hbar e^2}{2\pi m_e {c l_1}^2}\int_0^\infty d\nu\nu e^{-2\nu}\int_1^\infty \frac{dp}{p^2} \times \Phi'(\mathcal{R}_0^{\perp *}, \mathcal{R}_0^{\parallel *}, \mathcal{B}_0^*), \quad (4.85)$$

$$\Phi'(\mathcal{R}_0^{\perp *}, \mathcal{R}_0^{\parallel *}, \mathcal{B}_0^*) = 2\mathcal{B}_0^* + \left[\mathcal{R}_0^{\perp *} + \mathcal{R}_0^{\parallel *} - 2p^2(\mathcal{R}_0^{\parallel *} - \mathcal{B}_0^*)\right]. \quad (4.86)$$

where

TABLE I. Summary of some general results for the interactions between a polarizable system α and one wall (or one set of walls) or α and two walls (or two sets of walls). The conditions of validity and definitions are specified.

V	Conditions and definitions	Eq.
$V_{D_1\alpha D_2}$	arbitrary	(4.10)
$V_{D\alpha D}$	$\epsilon_3 = \epsilon_4 = \epsilon_5$, $d_1 = d_2 \equiv d, \epsilon_1 = \epsilon_2 \equiv \epsilon$	(4.21)
$V_{\mathcal{D}\alpha M}$	$d_1 = \infty, \epsilon_1 \sim 1, \epsilon_2 = \infty$	(4.20)
$V_{M\alpha M}$	$\epsilon_1 = \epsilon_2 = \infty$,	(4.43)
$V_{D_1\alpha}$	$d_2 = 0, \epsilon_3 = \epsilon_5$	(4.14)
$V_{D\alpha}$	$d_2 = 0, \epsilon_3 = \epsilon_4 = \epsilon_5$, $d_1 \equiv d, \epsilon_1 \equiv \epsilon$	(4.26)
$V_{M\alpha}$	$d_2 = 0, \epsilon_1 = \infty, \epsilon_3 = \epsilon_5$	(4.44)

For a thick wall we have

$$V_{Del}^{ret}|_{d\to\infty} = -\frac{\hbar e^2}{2\pi m_e c l_1^2}\Phi'(r_0^\perp, r_0^\parallel, \beta_0), \quad (4.88)$$

which was previously obtained [7]. The result for a thin wall is

$$V_{Del}^{ret}|_{d\sim 0} = \frac{\hbar e^2 d}{4\pi m_e c l_1^3}\phi, \quad (4.89)$$

TABLE II. Summary of the van der Waals and retardation interactions for wall-atom-wall, wall-electron-wall, wall-atom, and wall-electron systems in cases of finite, thick, and thin walls. The conditions of validity and definitions are specified in Table I. ϵ_3 is understood to be equal to unity for interactions involving an electron. References for the known results are included.

Interaction	van der Waals	Retardation
V_{DatD}	(4.38)	(4.29)
$V_{DatD}\|_{d\to\infty}$	(4.39)	(4.31)
$V_{DatD}\|_{d\sim 0}$	(4.41)	(4.33)
V_{DelD}		(4.74)
$V_{DelD}\|_{d\to\infty}$		(4.76)
$V_{DelD}\|_{d\sim 0}$		(4.77)
V_{MatM}	(4.50)[a]	(4.48)[a]
V_{MelM}	(4.83)[b]	(4.83)[b]
V_{Dat}	(4.54)	(4.53)
$V_{Dat}\|_{d\to\infty}$	(4.56)[c]	(4.55)[c]
$V_{Dat}\|_{d\sim 0}$	(4.58)	(4.57)
V_{Del}		(4.85)
$V_{Del}\|_{d\to\infty}$		(4.88)[d]
$V_{Del}\|_{d\sim 0}$		(4.89)
V_{Mat}	(4.60)[a]	(4.61)[e]
V_{Mel}	(4.90)[b]	(4.90)[b]

[a]Reference [16].
[b]Reference [6].
[c]Reference [5].
[d]Reference [7].
[e]Reference [4].

where ϕ in Eq. (4.89) is given by Eq. (4.78). The known interaction for an ideal wall [6]

$$V_{M\mathrm{el}} = \frac{\hbar e^2}{4\pi m_e c^2 l_1^2} \tag{4.90}$$

can also be obtained.

The various results obtained in this section are summarized in Table I for those of general types and in Table II for those in special limits.

F. Approximating a wall of finite thickness by one with $d = \infty$

In the above analyses of walls of finite thickness d, we obtained simplified limiting results for $d \sim 0$ and for $d \sim \infty$. We gave a qualitative discussion below Eq. (4.35) of the difference between a thin wall and a wall with $d \sim \infty$. It can be very desirable in the design and analysis of experiments to have a more quantitative estimate of the effects of having walls of finite d. We now give a few such estimates, but in a very limited context. We begin with the obvious remark that the effects of a wall are determined by its permittivity as well as by its thickness; an ideal wall of any d can be taken to have $d = \infty$, while a dilute wall would have to have d very large if it is to approximate a wall with $d = \infty$. We first look at the one-wall interaction given in Eq. (4.54).

For the short-range ($l_1 \sim 0$) wall-atom interaction, $\mathcal{B}$, defined in Eq. (4.36), can be approximated by

$$\mathcal{B} \approx \beta - \beta(1-\beta^2)e^{-2\nu d/l}, \tag{4.91}$$

where we expanded, retaining only the leading d-dependent term. Integrating over ν in Eq. (4.54) we find

$$V_{D\mathrm{at}}^{\mathrm{vdW}} \approx \frac{\hbar}{\pi l_1^3}\int_0^\infty d\xi \frac{\alpha}{\epsilon_3}\beta\left\{1 - \frac{1-\beta^2}{[1+(d/l_1)]^3}\right\}. \tag{4.92}$$

The first term in Eq. (4.92) is the thick-wall result $V_{D\mathrm{at}}^{\mathrm{vdW}}$ given in Eq. (4.56). If ϵ_3 and ϵ are of the same order, in which case β is of order unity, then the fractional error made in replacing $V_{D\mathrm{at}}^{\mathrm{vdW}}$ by $V_{D\mathrm{at}}^{\mathrm{vdW}}|_{d\to\infty}$ is of order

$$\frac{1}{[1+(d/l_1)]^3}. \tag{4.93}$$

If the fractional error is to be less than 10%, we must then have $d > 1.2l_1$. The lower bound on d will be somewhat reduced if ϵ_3 and ϵ are rather different.

A similar analysis can be applied to the long-range ($l_1 \sim \infty$) wall-atom interaction (4.53). We find the fractional error in replacing replacing $V_{D\mathrm{at}}^{\mathrm{vdW}}$ by $V_{D\mathrm{at}}^{\mathrm{vdW}}|_{d\to\infty}$ given in Eq. (4.55) to be roughly

$$\frac{1}{[(1+(d/l_1)]^4}. \tag{4.94}$$

For an error less than 10%, the lower limit of the thickness is about $d > 0.8l_1$. Applying the above analyses to the wall-electron system, we find that, for the retardation interaction, the thickness should be greater than $3.2l_1$. The lower bounds on d/l_1 may be a bit low. Thus $l_1 \sim 0$ implies that l_1 is much smaller than any relevant characteristic length, which here is d. The result $d > 0.8l_1$ for the long-range case is particularly suspect.

It was pointed out earlier that the interaction with two walls can be viewed as a converging sum of interactions with only one wall. [See Eq. (4.17) and the relevant discussion.] Hence the above analysis regarding the minimum thickness of the wall can be readily applied to the two-wall interactions. The analyses and bounds given above serve only as rough estimates on how thick a wall should be if it is to be considered as a thick wall. For accurate bounds and for bounds useful over the full interaction range, numerical calculations can be performed.

Some results on the deflection of atoms moving near the surface of a wall and subject to the nonretarded l^{-3} interaction were obtained about 20 years ago [17]. More recently, much more accurate results were obtained [18] for atom-wall separations in both the nonretarded and the retarded (l^{-4}) domains. These results are in very good agreement with the theoretical predictions.

ACKNOWLEDGMENT

The work was partially supported by National Science Foundation under Grant No. PHY 9400673.

[1] These include the interaction of two metallic walls [H. B. G. Casimir, Proc. K. Ned. Akad. Wet. **60**, 793 (1948)], of dielectric walls separated by a vacuum [E. M. Lifshitz, Sov. Phys. JETP **2**, 73 (1956)], and of dielectric walls separated by dielectric material [I. E. Dzyaloshinskii, E. M. Lifshitz, and L. Pitaevskii, Adv. Phys. **10**, 165 (1961)]. Two walls of finite thickness have been considered in the one-dimensional cases [D. Kupiszewska and J. Mostowski, Phys. Rev. A **41**, 4636 (1990); D. Kupiszewska, *ibid.* **46**, 2286 (1992)]. (For a metallic wall, the thickness is of course irrelevant.)

[2] A recent review is contained in P. W. Milonni, *The Quantum Vacuum* (Academic, New York, 1993).

[3] L. Spruch, in *Long Range Forces: Theory and Recent Experiments in Atomic Systems*, edited by F. S. Levin and D. Micha (Plenum, New York, 1992).

[4] H. B. G. Casimir and D. Polder, Proc. K. Ned. Akad. Wet. **60**, 793 (1948).

[5] E. M. Lifshitz, Sov. Phys. JETP **2**, 73 (1956).

[6] G. Barton, Proc. R. Soc. London Ser. A **320**, 320 (1970).

[7] Y. Tikochinsky and L. Spruch, Phys. Rev. A **48**, 4223 (1993).

[8] Y. Tikochinsky and L. Spruch, Phys. Rev. A **48**, 4236 (1993).
[9] L. H. Ford, Phys. Rev. A **48**, 2962 (1993).
[10] For its use in the evaluation of vacuum fluctuation fields, see N. G. Van Kampen, B. R. A. Nijboer, and K. Schram, Phys. Lett. **26A**, 307 (1968); K. Schram, *ibid.* **43A**, 283 (1973); D. Langbein, Solid State Commun. **12**, 853 (1973); see also Ref. [2] for a review.
[11] R. J. Glauber and M. Lewenstein, Phys. Rev. A **43**, 467 (1991).
[12] P. Candelas, Ann. Phys. (N.Y.) **143**, 241 (1982).
[13] D. Kupiszewska and J. Mostowski, Phys. Rev. A **41**, 4636 (1990); D. Kupiszewska, *ibid.* **46**, 2286 (1992).
[14] C. M. Hargreaves, Proc. K. Ned. Akad. Wet. Ser. B **68**, 231 (1965); J. Schwinger, L. L. DeRaad, Jr., and K. A. Milton, Ann. Phys. (N.Y.) **115**, 1 (1978); see also Ref. [2], p. 228.
[15] I. E. Dzyaloshinskii, E. M. Lifshitz, and L. Pitaevskii, Adv. Phys. **10**, 165 (1961).
[16] G. Barton, Proc. R. Soc. London Ser. A **410**, 141 (1987); **410**, 175 (1987).
[17] A. Shih and V. A. Parsegian, Phys. Rev. A **25**, 803 (1975).
[18] C. I. Sukenik, M. G. Boshier, D. Cho, V. Sandoghdar, and E. A. Hinds, Phys. Rev. Lett. **70**, 560 (1993).